

# Establishment of an in vitro 3D vascularized micro-tumor model and screening of chemotherapeutic drugs

**Qian Ye**

Anhui Medical University

**Juanru Wang**

First Affiliated Hospital of Anhui Medical University

**Boyang Wang**

Anhui Medical University

**Min Zhao**

Second People's Hospital of Hefei

**Zhengsheng Wu**

First Affiliated Hospital of Anhui Medical University

**Xiaoli Liu** (✉ [lxl\\_8512@163.com](mailto:lxl_8512@163.com))

Anhui Medical University

---

## Research Article

**Keywords:** breast cancer, three-dimensional culture, cell encapsulation, microcapsule, vasculogenesis

**Posted Date:** August 23rd, 2023

**DOI:** <https://doi.org/10.21203/rs.3.rs-3260252/v1>

**License:** © ⓘ This work is licensed under a Creative Commons Attribution 4.0 International License.

[Read Full License](#)

---

# Abstract

The three-dimensional (3D) cell culture system has received widespread attention in drug discovery, but current 3D culture models have limitations, and a simple and repeatable 3D culture model needs to be developed for high-throughput screening. In this study, we designed an encapsulation device to co-culture MCF-7 cells and HUVE cells in core-shell microcapsules. The formation of vascular lumen was determined by immunohistochemistry and immunofluorescence, and cell proliferation was detected by CCK-8 assay. Anticancer drugs (doxorubicin or paclitaxel) were added 12 hours after the 2D cultured cells were plated or 7 days after the cells grew in the core-shell microcapsules to observe the drug reactions between the models. We found that vascularized micro-tumors were successfully obtained after 14 days of 3D culture. Moreover, our study showed that the proliferation rate of 3D cultured cells was slower than that of 2D cultured cells. In addition, 3D cultured cells were more resistant to anticancer drugs than 2D cultured cells. In this study, we believe that the 3D culture model may provide an available platform for drug screening and is valuable for the study of tumor development and angiogenesis.

## 1. Introduction

For women, breast cancer (BC) is the most common type of cancer, accounting for about 31% of all new diagnoses[1]. In the process of drug discovery, the lack of efficacy and safety problems are the main reasons leading to the failure of clinical development phase[2]. Due to the high investment and low success rate in drug discovery, it is necessary to find new methods to improve the success rate of drug discovery. Two-dimensional (2D) cell cultures are the most commonly used *in vitro* methods for pre-clinical drug discovery, but they fail to mimic the real tumor microenvironment (TME) *in vivo*[3, 4]. Three-dimensional (3D) cell cultures are superior to 2D cell cultures in studying cell-cell and cell-matrix interactions[5]. Moreover, 3D tumor models can more accurately simulate the biological characteristics of solid tumors, such as cellular heterogeneity, gene expression, drug resistance, etc[4].

TME is a complex ecosystem full of heterogeneity, including cancer cells, stromal cells, blood vessels, nerve fibers, extracellular matrix (ECM) and related acellular components[6]. Stromal cells (including endothelial cells) may affect the sensitivity of cancer cells to anticancer drugs by modifying ECM and paracrine factors[7]. However, most 3D tumor models currently lack a vascular system. Due to diffusion limitations, living cells only exist within 200 $\mu$ m on the surface of 3D tumor models including spheroids[8].

Cell microencapsulation is a relatively new 3D culture technique that immobilizes well-functioning and living cells in a suitable matrix[9]. The appropriate matrix should mimic ECM, be biocompatible, and support cell survival. Alginate, collagen, fibrin, gelatin and hyaluronic acid are widely used natural polymer biomaterials because of their similarity to extracellular matrix components and can be used for cytotoxicity testing of various anticancer drugs in 3D cell models[10]. Sodium alginate is the most commonly used culture material, including (1,4) -linked  $\beta$ -d-mannose (M block) and  $\alpha$ -l-glucose acid blocks (G block), which can be crosslinked with divalent cations (such as  $\text{Ca}^{2+}$ ) to form hydrogels[11, 12]. Collagen, as the main component of ECM protein, has low antigenicity, low inflammatory reactivity and

biocompatibility, providing mechanical support for antagonistic forces[13, 14]. There are several methods for encapsulating cells into microcapsules, including electrostatic spraying, photolithography, emulsification and droplet microfluidics, but these fabrication processes are relatively complex and unsuitable for widespread use, and high efficiency is critical for future research[15, 16].

In this study, we designed a simple, reproducible and highly efficient microencapsulated device to co-culture MCF-7 cells and HUVE cells in microcapsules to establish an *in vitro* vascularized micro-tumor model for chemotherapeutic drug screening.

## 2. Materials and Methods

### 2.1 Cell Culture

MCF-7 cells (breast cancer cell line) and Human umbilical vein endothelial (HUVE) cells were donated by Professor Wu and Professor Zhao's laboratory, respectively. The Cells were cultured in dulbecco's modified eagle medium (DMEM, Gibco, USA) containing 10% fetal bovine serum (FBS, Gibco, USA) and 1% penicillin-streptomycin solution (Beyotime Biotechnology, Shanghai, China) and placed in a 5% humidified incubator at 37°C. The cells were digested from the culture flask using trypsin, centrifuged at 1200rpm/min for 5 minutes, the supernatant was discarded, and the cells were deposited on ice for later use.

### 2.2 Fabrication of Cell Encapsulation Device

The cell encapsulation device consisted of three different sizes of flat needles, including a purple needle with an inner diameter of 510µm, a pink needle with an inner diameter of 600µm, and a black needle with an inner diameter of 740µm. Firstly, the purple needle was placed inside the pink needle so that the two needles formed concentric circles in cross section. Then, the black needle vertically inserted in pink needle, and the three needles were bonded using hot melt adhesive as shown in Fig. 1. Next, the simple device was connected through the 'cross' scratch on the 1.5ml EP tube cover. Finally, the whole device was fixed in a 50ml centrifuge tube with a hollow foam.

### 2.3 Preparation of Core-Shell Microcapsules

Prior to the experiment, the cell encapsulation device was soaked in anhydrous ethanol and irradiated with UV light for 30 minutes, and then sterile saline was used to flush the device channels. The device has two microchannels, with inlet 1 as the core phase and inlet 2 as the shell phase. We mixed the neutralized rat tail tendon collagen type I (#C8062, Solarbio, China) at an initial concentration of 5mg/ml with MCF-7/HUVE cells (total density  $2 \times 10^6$  cells/ml), and added 2% sodium carboxymethyl cellulose to increase the hardness of ECM, finally kept the collagen concentration at 1.5mg/ml and injected into inlet 1. 2% sodium alginate or a mixture containing HUVE cells was injected from inlet 2. The outlet of the device was connected to a 1.5ml EP tube containing 0.1M CaCl<sub>2</sub> solution. All solutions were filtered using a 0.22µm needle filter.

Starting the centrifuge and adjusting the speed, sodium alginate will be gelatinized in  $\text{CaCl}_2$  solution to form microcapsules, and the collected microcapsules were transferred to complete medium containing EGM-2 cell culture factor (# CC-4176; Lonza, Switzerland) and cultured in a 5% $\text{CO}_2$  incubator at 37°C for 14 days.

## 2.4 Immunofluorescence

The cell-containing microcapsules were taken out after 1, 3, 5, and 7 days of culture, and Calcein AM/PI staining kit (Beyotime Biotechnology, Shanghai, China) was used to detect cell activity. Firstly, the Calcein AM/PI detection working fluid was prepared according to the instructions. Then, the microcapsules were washed with PBS, added with an appropriate amount of Calcein AM/PI detection working solution, and incubated at 37 ° C in dark for 30 minutes. Finally, the staining was observed using a fluorescence microscope.

The cell-containing microcapsules cells were taken out after 14 days of culture, and the shell (sodium alginate) was dissolved with 75mM sodium citrate to release micro-tumors. After washing with PBS for 3 times, the collected cell aggregates were transferred to a slide and fixed with 4% paraformaldehyde. After washing with PBS for 3 times, 0.5% Triton X-100 (Biosharp Life Sciences, Guangzhou, China) was added and incubated at room temperature for 15 minutes to increase the permeability of the cell membrane to the antibody. After washing with PBS, 2% BSA prepared with PBS was added and incubated at room temperature for 1 hour. Next, CD31 antibody with a dilution of 1: 100 (#11265-1-AP; proteintech, Wuhan, China) and actin antibody at a dilution of 1: 200 (# T0021; affinity Biosciences, USA) were added and incubated overnight at 4°C in a wet box. The next day, after washing 3 times with PBS, fluorescent secondary antibodies with a dilution of 1: 500 were added in the dark environment, including goat anti-mouse antibody coupled to DyLight 488 (# A23210; abbkine, USA) and goat anti-rabbit antibody conjugated to DyLight 594 (# A2 3420; abbkine, USA), incubated at 37°C in dark for 1 hour. Next, DAPI (Biosharp Life Sciences, Guangzhou, China) was added and incubated at room temperature for 10 minutes. After washing with PBS for 3 times, anti-fluorescence quenching agent was added dropwise and sealed. Finally, the staining was observed using a confocal microscope.

## 2.5 Immunohistochemistry

The cell-containing microcapsules were taken out after 2 weeks of culture, and the shell (sodium alginate) was dissolved with 75mM sodium citrate to release micro-tumors. After washing with PBS for 3 times, the collected cell aggregates were fixed with 4% paraformaldehyde for 24 hours. Then, the collected cell aggregates were dehydrated, embedded and prepared into 4 $\mu\text{m}$  paraffin sections. The paraffin sections were baked in a 65°C incubator for 2 hours, and dewaxed with xylene to water. The 0.01mol/L sodium citrate buffer was prepared and the antigenic sites were exposed by high-pressure thermal repair method. CD31 antibody (1:800; # 11265-1-AP; Protentech, Wuhan, China) was dripped and incubated overnight at 4 ° C. The next day, after washing PBS 3 times, an appropriate amount of Max Vision TM HRP polymer anti rabbit IHC kit (# Kit-5006; MXB Biotechnology, Fuzhou, China) were added, and incubated at room temperature for 15 minutes. After washing with PBS for 3 times, DAB staining

solution was added. Then, the slices were immersed in hematoxylin for staining, dehydrated and sealed. Finally, the imaging was observed using an optical microscope.

## 2.6 Proliferation Assay

As 3D culture groups, microcapsules containing MCF-7 cells, HUVE cells, and these two types of cells (1: 1) were inoculated on 96 well plates (100/well), and cultured in a complete medium containing EGM-2 cell culture factor. As 2D culture groups, MCF-7 cells, HUVE cells, and these two types of cells (1: 1) were inoculated in 96 well plates (500 cells/well), and cultured in a complete medium containing EGM-2 cell culture factor. On the 1st, 3rd, 5th and 7th day of culture, CCK-8 (Beyotime Biotechnology, Shanghai, China) reagent was used to measure the absorbance of cells at 450nm.

## 2.7 *In Vitro* Drug Response

Doxorubicin (DOX) was purchased from Keygen Biotech, Jiangsu, China (#KGA8184). Paclitaxel (PTX) was purchased from Solarbio Life Sciences, Beijing, China (#IP0020). Dimethyl sulfoxide (DMSO) was added to fully dissolve the drug to prepare a storage solution and stored at -80°C. Prior to the experiments, the drug was diluted with fresh medium at the appropriate concentration, with the final DMSO concentration was < 0.1%.

As 3D culture groups, microcapsules containing cells cultured for 1 week were inoculated in a 96 well plates (100/well), including microcapsules containing MCF-7 cells, HUVE cells and the two kinds of cells (1: 1). As 2D culture groups, MCF-7 cells, HUVE cells and two kinds of cells (1: 1) were inoculated in 96 well plates (5000 cells/well) and cultured for 12 hours. Then, the diluted DOX/PTX (0-100µg/ml) was added and incubated for 24 hours. The absorbance of the cells at 450nm was determined using CCK-8 reagent.

## 3. Results

### 3.1 Preparation of Core-Shell Microcapsules

The formation process of core-shell microcapsules is shown in Fig. 1. In the encapsulation process, it is very important to use hydrogels with appropriate viscosity, the most suitable viscosity is usually in the range of 300 – 30 000mPa ·s. The hydrogel solution with viscosity lower than 300mPa·s will lead to mechanical instability of the structure. Conversely, increasing the viscosity of the hydrogel ( $\leq 100000\text{mPa}\cdot\text{s}$ ) will bring mechanical integrity, but requires high pressure to squeeze the aqueous solution of the hydrogel, while cell viability and proliferation will decrease. The viscosity of different concentrations of sodium alginate was measured by a viscometer, and the results showed that 2% sodium alginate (4,050mPa·s) was more suitable for cell encapsulation (Fig. 2a). We collected the formed microcapsules for further observation and statistical analysis, and found that the microcapsules were homogeneous and their diameters were approximately normal distribution, with an average diameter of 444µm (Fig. 2b).

As shown in Fig. 2c, we compared the effects of three models on cell activity. The core of model A was a mixture of type I collagen and 2% sodium carboxymethyl cellulose (3: 6.5) containing MCF-7 cells and HUVE cells, and the shell was 2% sodium alginate. The core of model B was a mixture of type I collagen, 2% sodium carboxymethyl cellulose and 2% sodium alginate (3: 5.5: 1) containing MCF-7 cells and HUVE cells, and the shell was 2% sodium alginate. The core of model C was a mixture of type I collagen and 2% sodium carboxymethyl cellulose (3: 6.5) containing MCF-7 cells, and the shell was 2% sodium alginate containing HUVE cells. During the 1-week culture, cell activity was tested by sampling every 2 days. It was found that cells growing in a 3D microenvironment surrounded by matrix and gradually aggregated and maintained high activity (Fig. 2d-f). We also found that the cells in Model A had the lowest death rate and the greatest ability to aggregate.

**Fig 2.** Formation of core-shell microcapsules. (a) Viscosity of different concentrations of sodium alginate. (b) Normal distribution of microsphere size with a mean diameter of 444 $\mu$ m. (c) Schematic diagrams of the three different models. (d-f) Cell growth of microcapsules formed under Model A, Model B and Model C, respectively.

## 3.2 Formation of a 3D Vascularized Microtumor

We further observed the vascularization of micro-tumors in microcapsules produced by each of two models (A and C) under conventional static culture in 12-well plates. Since the cells in the microcapsules produced by Model B had a high mortality rate during culture, no further experiments were performed. The core of Model A was a mixture of type I collagen and 2% sodium carboxymethyl cellulose containing MCF-7 cells and HUVE cells (1: 1), and the shell was 2% sodium alginate. The core of Model C was a mixture of type I collagen and 2% sodium carboxymethyl cellulose containing MCF-7 cells, and the shell was 2% sodium alginate containing the same cell number of HUVE cells. The difference between the two models is whether there is direct cell–cell contact between MCF-7 cells and HUVE cells after encapsulation.

The microcapsules produced by the two models were transferred to complete medium containing EGM-2 cell culture factor, including cytokines such as vascular endothelial growth factor (VEGF), human fibroblast growth factor (hFGF), human endothelial growth factor (hEGF) and R3-insulin-like growth factor 1 (R3-IGF-1), to promote vasculogenesis and angiogenesis and then collected after two weeks of culture. The expression of CD31 in micro-tumor tissues was detected by immunohistochemistry and immunofluorescence. We observed that the microcapsules generated by both models had evident lumens formed by HUVE cells, as shown in Fig. 3a-b.

**Figure 3.** The formation of vascular lumen in micro-tumors. The micro-vascular lumen structure was observed by staining actin, CD31 and nuclei. (a) Micro-tumors formed by Model A. (b) Micro-tumors formed by Model C.

To study cell proliferation in the 3D engineered system, we selected Model A with low mortality, high aggregation and angiogenesis for further experiments. As shown in Fig. 4b-d, we observed that cell

proliferation in the 3D culture system was generally slower than that in the 2D culture system.

**Figure 4.** Cell proliferation in two-dimensional (2D) and three-dimensional (3D) culture. (a) Physical picture of cell proliferation in 3D culture. (b) Proliferation of mixed MCF-7 cells and HUVE cells in 2D and 3D culture. (c) Proliferation of MCF-7 cells in 2D and 3D culture. d) Proliferation of HUVECs in 2D and 3D culture. Scale bar = 50 $\mu$ m. (\*,  $P < 0.05$ ; \*\*,  $P < 0.01$ ; \*\*\*,  $P < 0.001$ )

### 3.3 *In Vitro* Drug Response

We compared the sensitivity of 2D and 3D cultured cells to chemotherapeutic drugs (DOX/PTX). As shown in Fig. 5a-f, 2D cultured cells were more sensitive to DOX and PTX. The average inhibitory concentration to achieve 50% cell killing (IC<sub>50</sub>) of free DOX was 8.79 $\mu$ g/ml and 20.82 $\mu$ g/ml in a mixture of MCF-7 cells and HUVE cells in 2D and 3D culture, respectively (a 1.3-fold increase). The IC<sub>50</sub> of free DOX in 3D culture (28.48 $\mu$ g/ml) of MCF-7 cells was 7.3 times that of 2D culture (3.89 $\mu$ g/ml), while the IC<sub>50</sub> of free DOX in 3D culture (148.82 $\mu$ g/ml) of HUVE cells was 8.7 times that of 2D culture (17.03 $\mu$ g/ml). In 2D and 3D culture, the IC<sub>50</sub> of free PTX in the mixture of MCF-7 cells and HUVE cells was 37.33 $\mu$ g/mL and 55.73 $\mu$ g/ml, respectively (a 0.4-fold increase). The IC<sub>50</sub> of free PTX in 3D culture (78.80 $\mu$ g/ml) of MCF-7 cells was 2.6 times that in 2D culture (29.23 $\mu$ g/ml), while the IC<sub>50</sub> of free PTX in 3D culture (144.23 $\mu$ g/ml) of HUVE cells was 4.3 times that in 2D culture (32.81 $\mu$ g/ml).

**Figure 5.** The sensitivity of 2D and 3D cultured cells to chemotherapeutic drugs. (a) Survival curves of the mixed MCF-7 cells and HUVE cells after doxorubicin (DOX) treatment and the IC<sub>50</sub> values. (b) Survival curves of MCF-7 cells after DOX treatment and the IC<sub>50</sub> values. (c) Survival curves of HUVE cells after DOX treatment and the IC<sub>50</sub> values. (d) Survival curves of the mixed MCF-7 cells and HUVECs after paclitaxel (PTX) treatment and the IC<sub>50</sub> values. (e) Survival curves of MCF-7 cells after PTX treatment and the IC<sub>50</sub> values. (f) Survival curves of HUVECs after PTX treatment and the IC<sub>50</sub> values. (\*,  $P < 0.05$ ; \*\*,  $P < 0.01$ ; \*\*\*,  $P < 0.001$ )

In the tested cell lines, there was a significant difference in sensitivity between 2D culture and 3D culture. These findings demonstrated that the dimension of the culture model affects the sensitivity of tumor cells to anticancer drugs.

## 4. Discussion

3D cell cultures have gained increasing attention in drug screening. However, many current available 3D culture techniques cannot be widely used due to time-consuming, expensive and lack of repeatability. In this study, we designed a simple, reproducible and efficient cell encapsulation device by which MCF-7 cells and HUVE cells were encapsulated in semi-permeable hydrogels. Although the biocompatibility of sodium alginate has been widely studied, the effect of alginate composition on its biocompatibility is a controversial issue. The residual impurities in sodium alginate are the main causes of poor biocompatibility, foreign body reaction and inflammatory response[17]. The use of purified sodium alginate can reduce the potential immune response of the host[18]. This is consistent with our

experimental results. We found that cells encapsulated in hydrogels containing sodium alginate appeared to have higher mortality and poorer cohesion. Therefore, we used collagen with low antigenicity as the core and add sodium carboxymethyl cellulose to increase the viscosity of the solution. This method achieves good biocompatibility and suitable porous structure for efficient cell attachment with good cell activity, proliferation and extracellular matrix remodeling.

Angiogenesis can promote the development and progression of tumors, while solid tumors require blood vessels to grow[19, 20]. During angiogenesis, endothelial cells respond to growth signals (e.g., basic fibroblast growth factor (bFGF), VEGF) to proliferate and migrate to form new blood vessels[20, 21]. Although several growth factors play a role in angiogenesis, VEGF is the most effective angiogenesis stimulator[22]. Cancer cells in 3D microtumors can release VEGF to activate the VEGF / VEGFR signaling pathway, which plays a crucial role in angiogenesis and tumor growth[7, 23]. Therefore, we cultured the generated microcapsules in medium supplemented with endothelial cell growth factors, including VEGF, hFGF-B, R3-IGF-1 and hEGF. After 14 days of culture, the expression of CD31 was detected by immunofluorescence and immunohistochemistry, and HUVE cells were found to form tubular lumens in the micro-tumor tissues. These results indicated that we successfully constructed *in vitro* 3D vascularized micro-tumors.

A large amount of evidence suggests that the growth rate difference between 2D monolayer and 3D culture systems depends on cell line and ECM[24]. Anna et al. found that the proliferation of colorectal cancer (CRC) cell lines in laminin-rich extracellular matrix (lrECM) was significantly reduced[25]. In addition, Vesa et al. showed that the growth rate of JIMT1 cells cultured in Matrigel was 1.86-fold faster than that of 2D monolayer culture. Interestingly, the growth rate of the same cell in poly-2-hydroxyethyl methacrylate (poly-HEMA) was 7.2-fold slower than that of 2D monolayer culture[26]. Our results indicated that the growth rate of cells in 3D culture (model A) was slower than that in 2D monolayer culture.

Many studies have found that 2D and 3D cultured cells have different responses to anticancer drugs, and 3D cultured cells have lower sensitivity to anticancer drugs[27, 28]. Compared with *in vivo* tumors, 2D cultured tumor cells *in vitro* exhibit slower tumor progression and lower drug resistance, leading to lower efficiency of drug screening and testing[29]. Yoshinori et al. found that different BC cell lines have different sensitivity to PTX and DOX[30]. In 3D culture, dense multicellular spheroids formed by BT-549, BT-474 and T-47D showed stronger resistance, while loose multicellular spheroids formed by MCF-7, HCC-1954 and MDA-MB-231 showed similar sensitivity to 2D culture. Our current study found that the resistance index (RI) of 3D cultured cells to anticancer drugs (DOX and PTX) was 1.49 to 8.73 times that of 2D cultured cells. This further indicates that TME has a significant effect on cell drug resistance, but the mechanism of drug resistance in this 3D culture model is still unclear and needs further exploration and research.

## 5. Conclusions

In summary, we demonstrated the ability this sample encapsulation device to form core-shell microcapsules and successfully constructed 3D vascularized micro-tumors *in vitro*. In addition, our study showed that 3D cultured cells had slower proliferation rate and higher drug resistance than 2D cultured cells. Therefore, the 3D culture model may be valuable for studying the mechanism of tumor angiogenesis, drug resistance of tumor cells and screening anticancer drugs.

## Declarations

**Author Contributions:** Conceptualization, Q.Y. and X.L.L.; Data curation, Q.Y., J.R.W. and X.L.L.; Formal analysis, Q.Y., X.L.L. and Z.S.W.; Funding acquisition, M.Z., Z.S.W. and X.L.L.; Investigation, Q.Y., J.R.W., B.Y.W., M.Z., Z.S.W. and X.L.L.; Methodology, Q.Y. and X.L.L.; Project administration, X.L.L.; Resources, M.Z., Z.S.W. and X.L.L.; Supervision, X.L.L.; Validation, Q.Y. and J.R.W.; Visualization, Q.Y., J.R.W. and X.L.L.; Writing—original draft, Q.Y. and X.L.L.; Writing—review and editing, Q.Y., J.R.W., B.Y.W., M.Z., Z.S.W. and X.L.L.. All authors have read and agreed to the published version of the manuscript.

**Funding:** This study was supported by Basic and Clinical Cooperative Research Promotion Program of Anhui Medical University (No. 2020xkjT012), BSKY Scientific Research Project of Anhui Medical University (No. XJ201801) and Applied Medical Research Project of Hefei Health Commission (No. Hwk2021yb012).

**Data Availability Statement:** All data generated or analyzed during this study are included in the manuscript. Further inquiries should be directed to the corresponding author.

**Acknowledgments:** We thank Professor Zhao Gang (CryoBME & Micro-Nano-Bio- Systems Engineering Laboratory, University of Science and Technology of China, China) for the generous gift of HUVE cells, as well as Professor Wu Qiang (Pathology Laboratory, Anhui Medical University, China) for the generous gift of MCF-7 cells.

**Conflicts of Interest:** The authors declare no conflict of interest. The funders had no role in the design of the study; in the collection, analyses, or interpretation of data; in the writing of the manuscript; or in the decision to publish the results.

## References

1. Siegel RL, Miller KD, Fuchs HE, Jemal A. Cancer statistics, 2022. *Cancer J Clin.* 2022;72(1):7–33.
2. Arrowsmith J, Miller P. Trial watch: phase II and phase III attrition rates 2011–2012. *Nat Rev Drug Discovery.* 2013;12(8):569.
3. Breslin S, O'Driscoll L. Three-dimensional cell culture: the missing link in drug discovery. *Drug Discovery Today* 2013.
4. Costa EC, Moreira AF, Melo-Diogo DD, Gaspar VM, Carvalho MP, Correia IJ. 3D tumor spheroids: an overview on the tools and techniques used for their analysis. *Biotechnol Adv* 2016:1427.

5. Habanjar O, Diab-Assaf M, Caldefie-Chezet F, Delort L. 3D Cell Culture Systems: Tumor Application, Advantages, and Disadvantages. *Int J Mol Sci* 2021, 22(22).
6. Jin MZ, Jin WL. The updated landscape of tumor microenvironment and drug repurposing. *Signal Transduct Target therapy*. 2020;5(1):166.
7. Agarwal P, Wang H, Sun M, Xu J, Zhao S, Liu Z, Gooch KJ, Zhao Y, Lu X, He X. Microfluidics Enabled Bottom-Up Engineering of 3D Vascularized Tumor for Drug Discovery. *ACS Nano* 2017:acs.nano7b00824.
8. Zhang W, Zhao S, Rao W, Snyder J, Choi JK, Wang J, Khan IA, Saleh NB, Mohler PJ, Yu J. a novel core-shell microcapsule for encapsulation and 3d culture of embryonic stem cells. 2019.
9. Kang SM, Lee JH, Yun SH, Takayama S. Alginate Microencapsulation for Three-Dimensional In Vitro Cell Culture. *ACS Biomaterials Science and Engineering* 2020.
10. Langhans SA. Three-Dimensional in Vitro Cell Culture Models in Drug Discovery and Drug Repositioning. *Front Pharmacol*. 2018;9:6–.
11. Mooney M. Alginate hydrogels as synthetic extracellular matrix materials. *Biomaterials* 1999.
12. Gasperini L, Mano JF, Reis RL. Natural polymers for the microencapsulation of cells. *J Royal Soc Interface*. 2014;11(100):20140817.
13. Catoira MC, Fusaro L, Di Francesco D, Ramella M, Boccafoschi F. Overview of natural hydrogels for regenerative medicine applications. *J Mater Sci - Mater Med*. 2019;30(10):115.
14. Vazquez-Portalatin N, Alfonso-Garcia A, Liu JC, Marcu L, Panitch A. Physical, Biomechanical, and Optical Characterization of Collagen and Elastin Blend Hydrogels. *Ann Biomed Eng*. 2020;48(12):2924–35.
15. Argenti S, Siciliano P, Blasi L. How Microgels Can Improve the Impact of Organ-on-Chip and Microfluidic Devices for 3D Culture: Compartmentalization, Single Cell Encapsulation and Control on Cell Fate. *Polymers*; 2021.
16. Agarwal P, Zhao S, Bielecki P, Rao W, Choi JK, Zhao Y, Yu J, Zhang W, He X. One-step microfluidic generation of pre-hatching embryo-like core-shell microcapsules for miniaturized 3D culture of pluripotent stem cells. *Lab Chip*. 2013;13(23):4525–33.
17. Orive G, Carcaboso AM, Hernandez RM, Gascen AR, Pedraz JL. Biocompatibility Evaluation of Different Alginates and Alginate-Based Microcapsules.
18. Lee J, Lee KY. Local and Sustained Vascular Endothelial Growth Factor Delivery for Angiogenesis Using an Injectable System. *Pharm Res*. 2009;26(7):1739–44.
19. Trédan O, Lacroix-Triki M, Guiu S, Mouret-Reynier MA, Barrière J, Bidard FC, Braccini AL, Mir O, Villanueva C, Barthélémy P. Angiogenesis and tumor microenvironment: bevacizumab in the breast cancer model. *Target Oncol* 2015.
20. Li Y, Zhu H, Wei X, Li H, Yu Z, Zhang H, Liu W. LPS induces HUVEC angiogenesis in vitro through miR-146a-mediated TGF- $\beta$ 1 inhibition. *Am J translational Res*. 2017;9(2):591–600.

21. Goto F, Goto K, Weindel K, Folkman J. Synergistic effects of vascular endothelial growth factor and basic fibroblast growth factor on the proliferation and cord formation of bovine capillary endothelial cells within collagen gels. *Lab Invest*. 1993;69(5):508–17.
22. Ferrara N, Gerber HP, Lecouter J. The biology of VEGF and its receptors. *Nat Med*. 2003;9(6):669–76.
23. Karaman S, Leppanen V-M, Alitalo, Kari: Vascular endothelial growth factor signaling in development and disease. *Development* 2018.
24. Edmondson R, Broglie JJ, Adcock AF, Yang L. Three-dimensional cell culture systems and their applications in drug discovery and cell-based biosensors. *Assay Drug Dev Technol*. 2014;12(4):207–18.
25. Luca AC, Sabrina M, René D, Stephan S, Isabelle M, Karl-Ludwig SF, Baldus SE, Wolfgang H, Piekorz RP, Knoefel WT. Impact of the 3D Microenvironment on Phenotype, Gene Expression, and EGFR Inhibition of Colorectal Cancer Cell Lines. *PLoS ONE*. 2013;8(3):e59689.
26. Vesa H, Sandra JM, Vidal F, John-Patrick M, Kristine KS, Olli K, Merja PL. Maria?A. D: High-Throughput 3D Screening Reveals Differences in Drug Sensitivities between Culture Models of JIMT1 Breast Cancer Cells. *PLoS ONE*. 2013;8(10):e77232.
27. Loessner D, Stok KS, Lutolf MP, Hutmacher DW, Clements JA, Rizzi SC. Bioengineered 3D platform to explore cell-ECM interactions and drug resistance of epithelial ovarian cancer cells. *Biomaterials*. 2010;31(32):8494–506.
28. Karlsson H, Frykn?S MR, Larsson R, Nygren P. Loss of cancer drug activity in colon cancer HCT-116 cells during spheroid formation in a new 3-D spheroid cell culture system. *Exp Cell Res*. 2012;318(13):1577–85.
29. Huang L, Abdalla AME, Xiao L, Yang G. Biopolymer-Based Microcarriers for Three-Dimensional Cell Culture and Engineered Tissue Formation. *Int J Mol Sci*. 2020;21(5):1895.
30. YOSHINORI IMAMURA, TORU, MUKOHARA, YOHEI, SHIMONO, YOHEI, FUNAKOSHI, NAOKO CHAYAHARA. Comparison of 2D- and 3D-culture models as drug-testing platforms in breast cancer. *Oncol Rep* 2015, 33(4).

## Figures

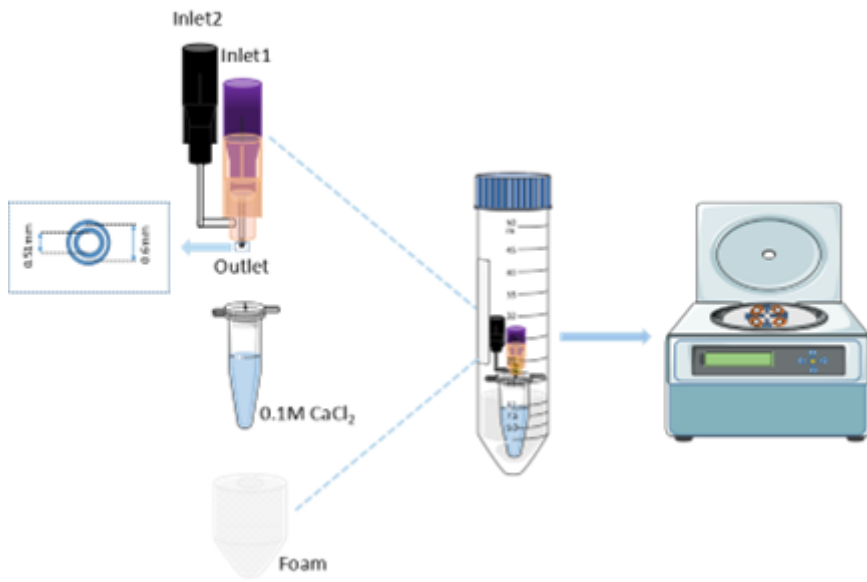


**Figure 1**

The schematic diagram of encapsulation device for forming core-shell microcapsules.

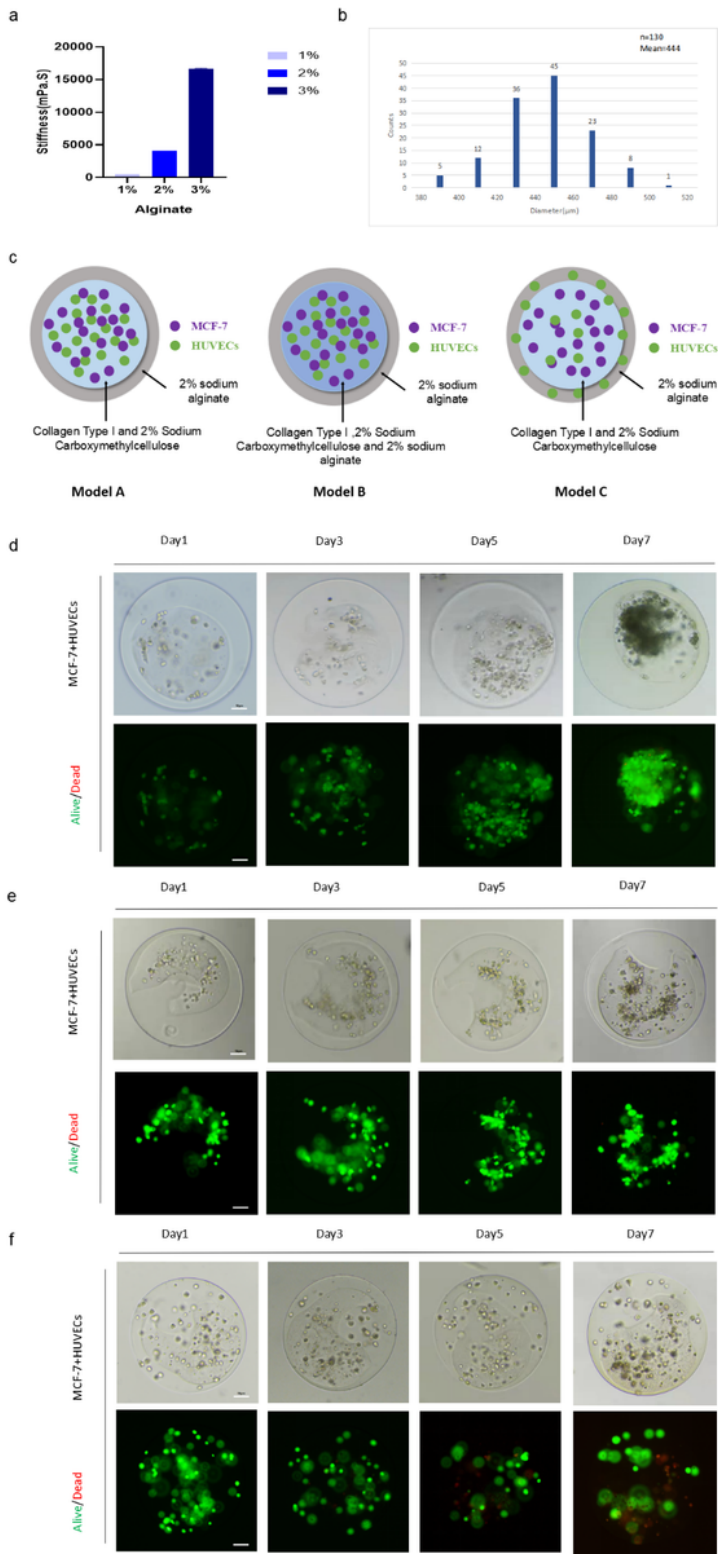


**Figure 2**

Formation of core-shell microcapsules. (a) Viscosity of different concentrations of sodium alginate. (b) Normal distribution of microsphere size with a mean diameter of 444µm. (c) Schematic diagrams of the three different models. (d-f) Cell growth of microcapsules formed under Model A, Model B and Model C, respectively.

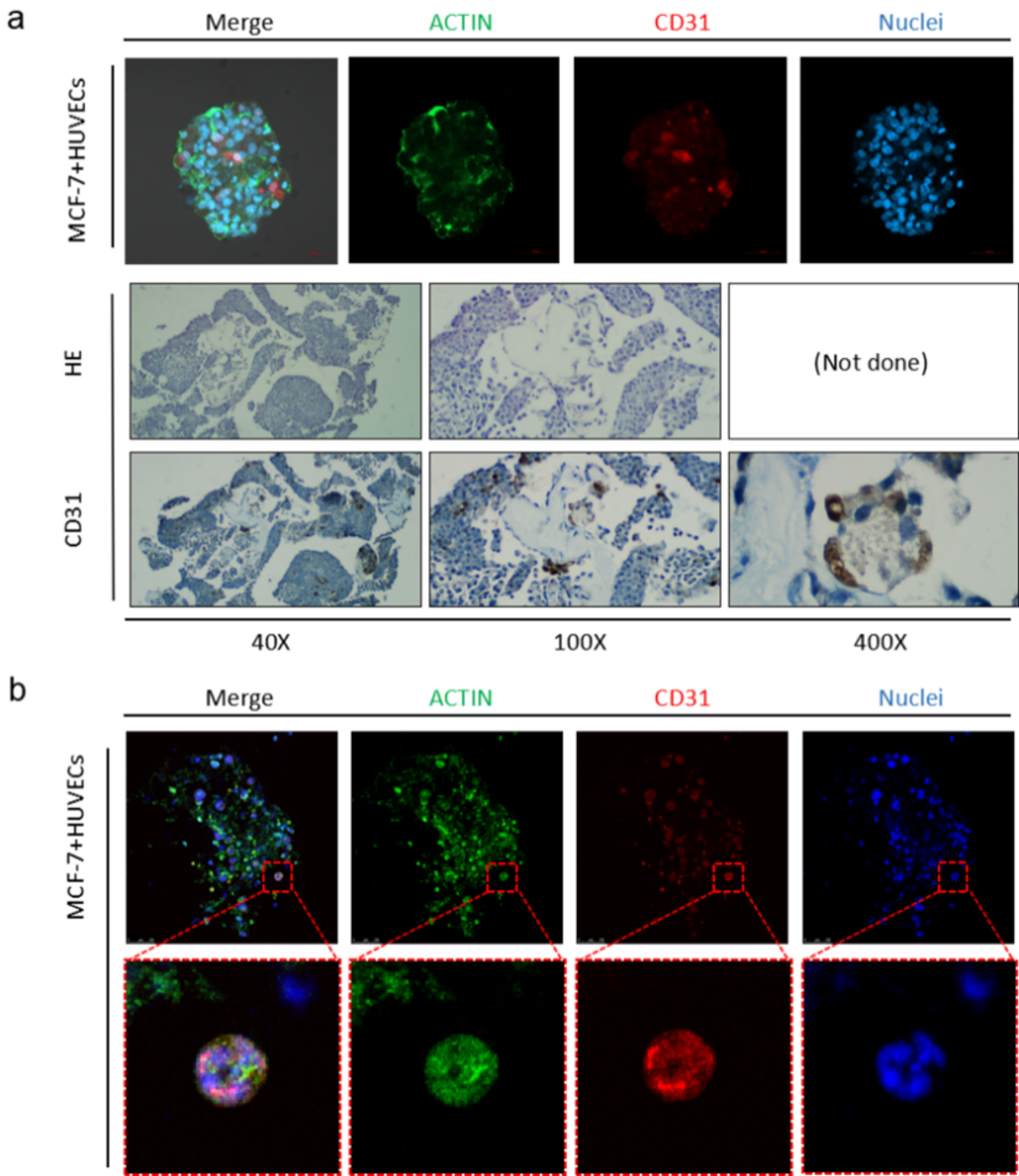


**Figure 3**

The formation of vascular lumen in micro-tumors. The micro-vascular lumen structure was observed by staining actin, CD31 and nuclei. (a) Micro-tumors formed by Model A. (b) Micro-tumors formed by Model C.

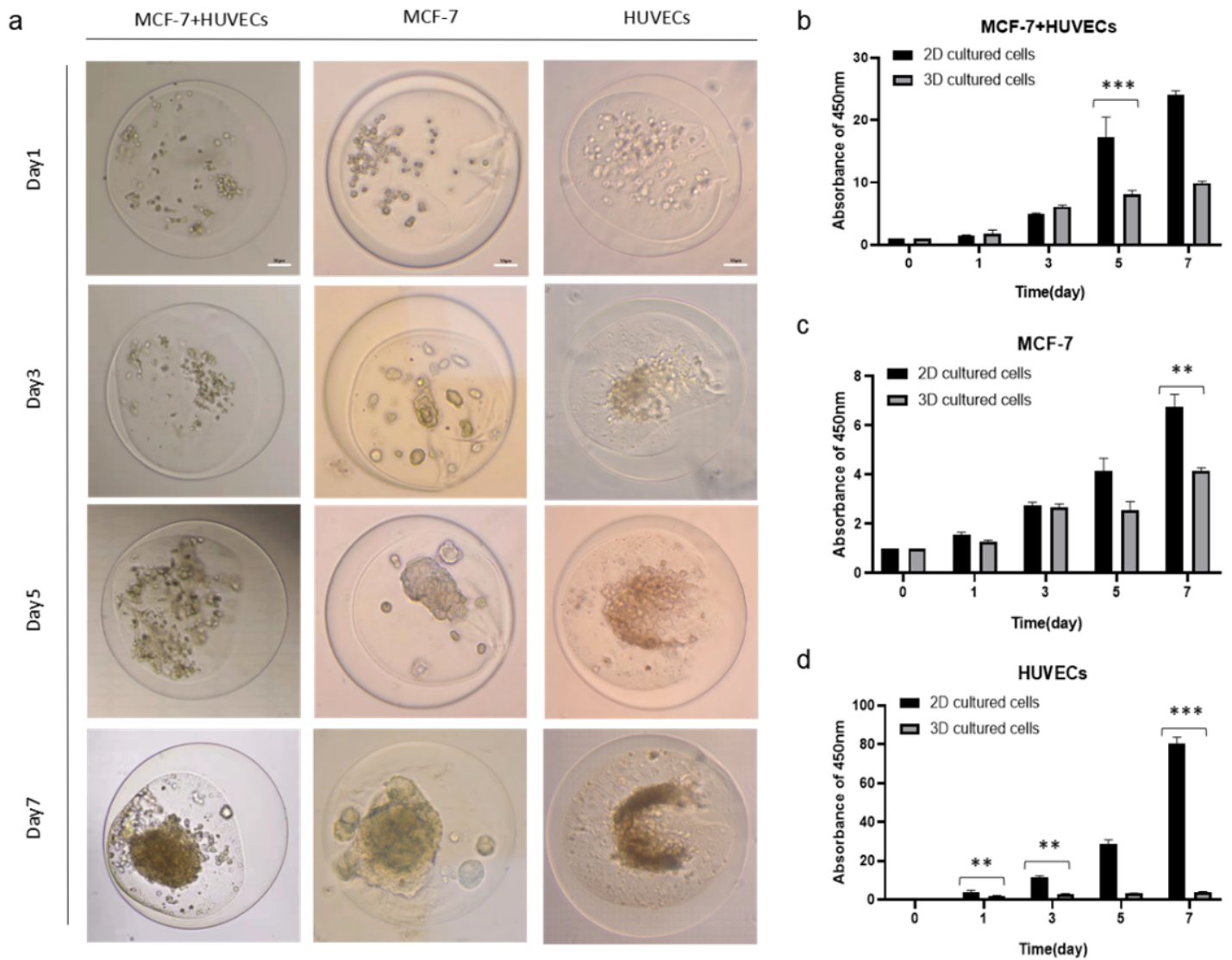


**Figure 4**

Cell proliferation in two-dimensional (2D) and three-dimensional (3D) culture. (a) Physical picture of cell proliferation in 3D culture. (b) Proliferation of mixed MCF-7 cells and HUVE cells in 2D and 3D culture. (c) Proliferation of MCF-7 cells in 2D and 3D culture. (d) Proliferation of HUVECs in 2D and 3D culture. Scale bar = 50 $\mu$ m. (\*,  $P < 0.05$ ; \*\*,  $P < 0.01$ ; \*\*\*,  $P < 0.001$ )

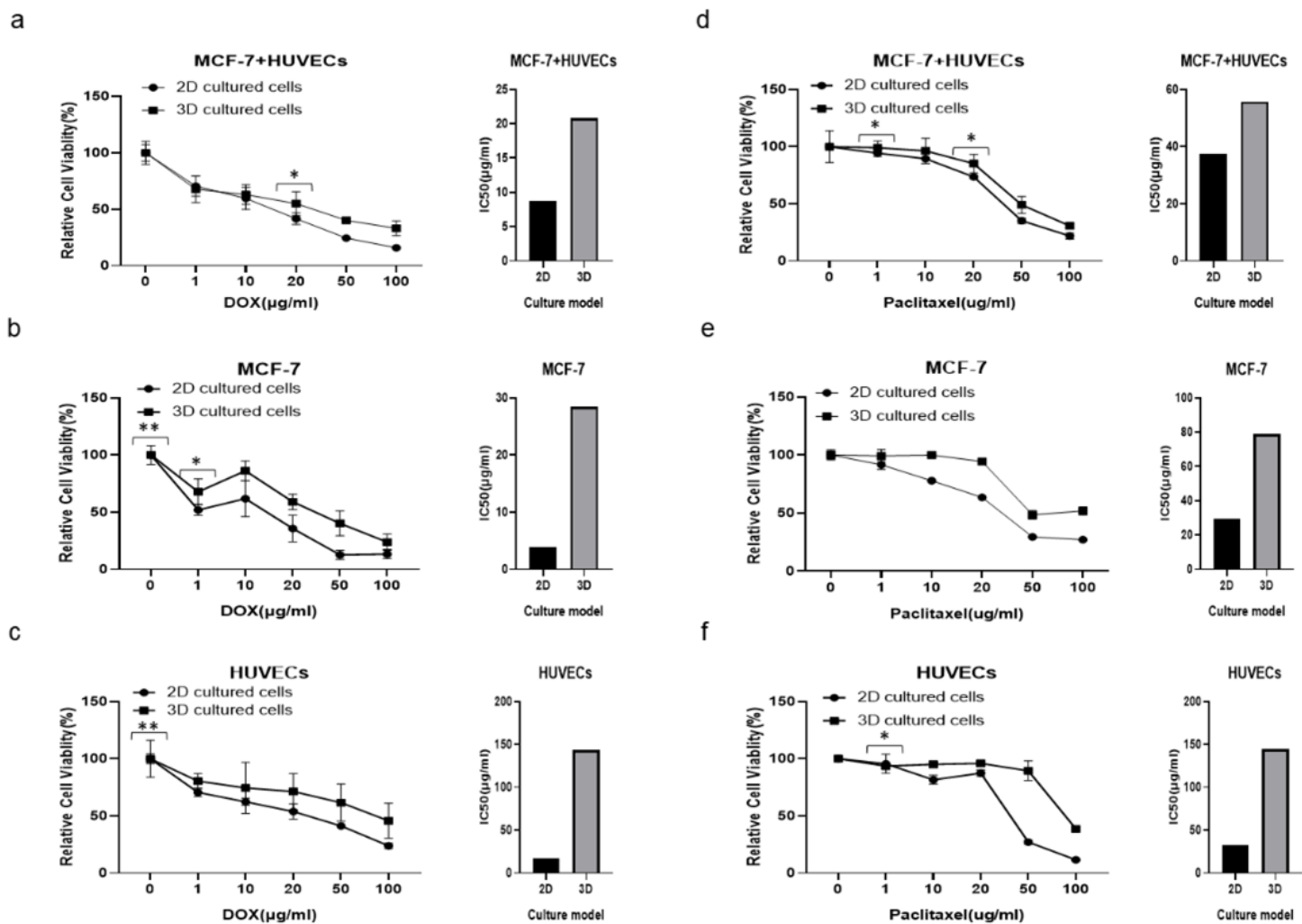


**Figure 5**

The sensitivity of 2D and 3D cultured cells to chemotherapeutic drugs. (a) Survival curves of the mixed MCF-7 cells and HUVE cells after doxorubicin (DOX) treatment and the IC<sub>50</sub> values. (b) Survival curves of MCF-7 cells after DOX treatment and the IC<sub>50</sub> values. (c) Survival curves of HUVE cells after DOX treatment and the IC<sub>50</sub> values. (d) Survival curves of the mixed MCF-7 cells and HUVECs after paclitaxel (PTX) treatment and the IC<sub>50</sub> values. (e) Survival curves of MCF-7 cells after PTX treatment and the IC<sub>50</sub> values. (f) Survival curves of HUVECs after PTX treatment and the IC<sub>50</sub> values. (\*, P < 0.05; \*\*, P < 0.01; \*\*\*, P < 0.001)

## Supplementary Files

This is a list of supplementary files associated with this preprint. Click to download.

- [GraphicalAbstract.png](#)